
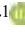
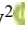




Flow Modeling for Hybrid Solar Chimney System Optimization Using Nozzle and Canopy

Hyder M. Abdul Hussein^{1*}, Nasr A. Jabbar¹, Ahmed R. Zainy²

¹ Department of Mechanical Engineering, Faculty of Engineering, University of Kufa, Najaf 54001, Iraq

² Basic Science Department, Faculty of Dentistry, University of Kufa, Najaf 54001, Iraq

Corresponding Author Email: hyderm.alabady@uokufa.edu.iq

Copyright: ©2025 The authors. This article is published by IIETA and is licensed under the CC BY 4.0 license (<http://creativecommons.org/licenses/by/4.0/>).

<https://doi.org/10.18280/ijht.430432>

ABSTRACT

Received: 17 June 2025

Revised: 3 August 2025

Accepted: 12 August 2025

Available online: 31 August 2025

Keywords:

hybrid solar chimney, solar updraft power, nozzle, renewable energy, computational fluid dynamics

This study presents a computational investigation of a hybrid solar chimney (HSC) system optimized through the introduction of internal geometric modifications—specifically, a nozzle, a canopy, and a combined nozzle-canopy design. The objective is to enhance natural ventilation and increase power output by improving airflow dynamics and thermal performance. Using Computational Fluid Dynamics (CFD), three modified HSC models were analyzed and compared to a validated baseline case. The results indicate that the nozzle increases axial velocity and improves the conversion of thermal energy to kinetic energy, while the canopy stabilizes and directs the updraft, enhancing flow coherence. The combined model achieved the highest performance, with a maximum air velocity of 4.18 m/s and a power output increase of over 80% compared to the conventional design. Temperature contours revealed improved thermal stratification and energy retention, particularly along the chimney centerline. The findings confirm that integrating both nozzle and canopy structures into the chimney design significantly enhances system efficiency, providing practical insights for sustainable building ventilation and solar energy utilization.

1. INTRODUCTION

The global energy sector is undergoing a fundamental transition toward renewable resources as a means of reducing dependence on fossil fuels and mitigating climate change. Among these alternatives, solar energy has emerged as one of the most promising options due to its abundance, sustainability, and potential to support the growing demand for clean electricity. Projections by the International Energy Agency suggest that solar power could become the world's largest source of electricity by 2050, contributing over one-third of global production. Despite these prospects, the widespread use of solar energy is constrained by intermittency, high initial investment, and the relatively modest efficiency of current technologies.

In parallel, buildings responsible for a substantial share of global energy use through heating, cooling, ventilation, and lighting are increasingly targeted for energy conservation strategies. Solar chimneys, also known as solar updraft towers, represent an effective passive system that simultaneously enhances natural ventilation and generates renewable energy. However, conventional solar chimney designs are often limited by low airflow velocity and insufficient power output, which restricts their scalability and broader application. Hybrid solar chimney (HSC) systems have been developed as an advanced alternative, combining solar thermal collection with photovoltaic integration to improve efficiency and multifunctionality. Although recent research has introduced various modifications—including structural changes, hybridization with auxiliary systems, and material

enhancements further design optimization is necessary to overcome the challenges of cost, system complexity, and performance under variable environmental conditions. Iraq aims to install 12GW of solar photovoltaic capacity by 2030, representing approximately 25% of the country's total power generation capacity [1]. In this context, energy conservation, demand-reduction strategies, and the use of renewable resources have gained increasing attention. Energy consumption in buildings primarily arises from ventilation, heating, cooling, and lighting. Among these, ventilation plays a vital role as it directly influences occupants' comfort and health [2-5]. Despite advancements, solar energy systems continue to face efficiency limitations, motivating efforts to enhance their performance. Solar chimneys, also referred to as solar updraft towers, are one such technology developed to harness solar energy for electricity generation [6, 7].

A HSC offers a promising approach to enhancing sustainability in both the energy and construction sectors. Figure 1 illustrates its general operation, showing how air enters from the lower surface and rises toward the central chimney section.

While all of these sources can be utilized, achieving this depends largely on the geographical location and time conditions to design robust systems that utilize these resources as efficiently as possible [8-10]. Despite recent advances in improving renewable energy technologies, studies indicate that utilization rates and efficiency are still generally below the desired level. Therefore, this study focuses on solar and wind energy in particular, given their direct relevance to the current research objectives. Solar energy is one of the most promising

solutions to the global challenges of fossil fuel depletion and climate change, as it is a clean, renewable and virtually unlimited source [11, 12]. According to the International Energy Agency (IEA), solar energy is expected to become the world's most important source of electricity by 2050, contributing more than 33% of total production [13].

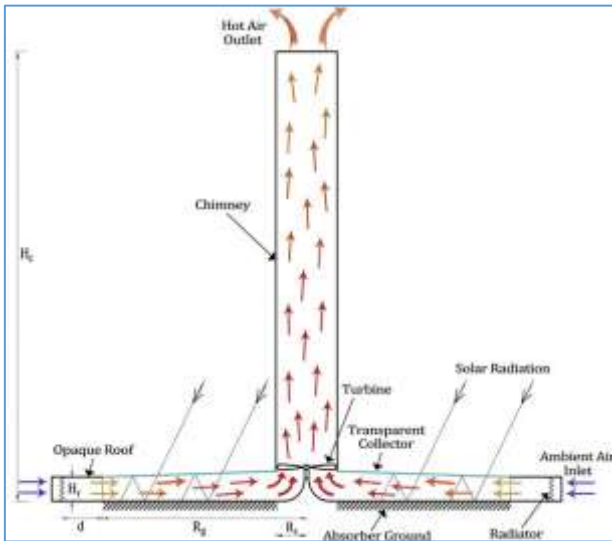


Figure 1. General diagram of the hybrid solar inlet system [8]

However, the uses of solar energy face challenges such as the high initial cost of equipment and its dependence on weather conditions [14, 15]. Furthermore, recent technological advances in energy storage (such as advanced batteries) and improved solar cell efficiency (which has exceeded 22% in some technologies) are beginning to reduce these barriers [16, 17]. Recent studies suggest that investing in solar energy could radically transform the energy sector, especially as its cost has fallen by 82% between 2010 and 2020, making it a strong competitor to conventional fuels [18]. Estimated by IRENA using a range of data sources, the total amount of renewable energy in 2024 was 1599 MW, of which 42 MW came from solar energy [19]. The installed capacity of solar electricity, including the locations of individual solar farms, is less than 0.1 GW [20, 21]. Moreover, the HSC is an innovative development that combines solar thermal and photovoltaic technologies to enhance ventilation efficiency of the system and generate energy simultaneously. While a conventional solar chimney relies on heating the air with solar radiation to stimulate natural ventilation, the hybrid version integrates photovoltaic (PV) panels on the chimney's exterior surfaces, allowing excess solar radiation to be converted into electricity [22]. This integration enables the system to achieve two purposes: Improve ventilation through upward air currents, and generate clean energy to support the needs of the building or the local grid [8]. The most important of this HSC trend is that the initial construction cost and the design of complex hybrid systems are still major obstacles, especially in resource-limited areas [23].

Ghorbani et al. [24] prepares a novel design that integrates a tower of dry cooling and a solar chimney to enhance thermal effectiveness on the Shahid Rajaei 250 MW power plant of steam in Iran, employing a numerical finite volume method to analyze various dimension parameters of a hybrid cooling tower. The design optimizations resulted in a power output ranging from 360 kW to over 4.4 MW, leading to a maximum

thermal efficiency increase of 0.538%. Zou and He [25] developed a three-dimensions model to compare the performance of Hybrid Cooling Tower–Solar Chimney (HCTSC), and natural draft dry cooling towers in terms of turbine power output and heat dissipation. Although the power production is more than 20 times that of a conventional solar chimney, the heat dissipation capacity is compromised. This can be regained to increase the heat exchanger's surface area for heat transfer.

Al-Kayiem et al. [26] proposed a HSC system enhanced with flue gas thermal channels to enable continuous power generation, including at night. A prototype with a 6 m collector and 6.65 m chimney was tested and simulated using ANSYS-Fluent. Validation showed good agreement with experimental data. Without flue gas, airflow and temperature rose by 6.87% and 6.3%. With flue gas at 116°C, mass flow and efficiency of collector improved by 12% and 64%, respectively. The study confirms the hybrid design significantly boosts performance and supports 24/7 operation. Hou et al. [27] examined the effectiveness of solar chimneys in enhancing natural ventilation by analyzing airflow behavior with varying gap-to-height ratios (0.1-0.5). A reverse flow was detected at the outlet when the gap reached 400 mm, adversely affecting airflow. The findings reveal nonuniform temperature and velocity distribution within the chimney, complicating airflow prediction.

Abdelsalam et al. [28] used a year's weather data from Aqaba, Jordan, the hybrid solar chimney power plant (HSCPP) produced 528 MWh/year 50% more electricity than a standard solar chimney power plant (SCPP) and desalinated 138,300 m³ of seawater annually, 1.5 times higher than the traditional system. It also cut CO₂ emissions by 40% and improved efficiency by 1.4 times, offering a sustainable, economically viable solution for water and energy production. Nugroho and Ahmad [29] demonstrated that integrating passive strategies like solar chimneys and vertical greenery can effectively reduce indoor temperatures by up to 5.5°C in tropical climates, enhancing natural ventilation and maintaining thermal comfort without mechanical cooling. Moosavi et al. [30] developed a passive cooling strategy incorporating a solar chimney, windcatcher, and system for water spraying to enhance natural ventilation in a two-storey building. Numerical simulations supported by experimental validation demonstrated the effectiveness of the integrated system in improving airflow and reducing indoor temperature. The implementation of the water spray and windcatcher led to a rate indoor temperature reduction of 5.2°C and achieved a peak air change rate of 9 ACH. On the hottest summer days, the system reduced energy consumption for ventilation and cooling by 90% and 75%, respectively. A new approach to increase the efficiency of the solar chimney using PV panels was proposed by Singh et al. [31]. The results indicated that the chimney outlet to inlet radius ratio, R_{co}/R_c (CORR) ratio and collector inlet changed, and that the most effective area for cooling solar cells is about 80% of the collector area evaluated from the center of the system tower. Additionally, the shape of the chimney tower and solar collector was modified, which resulted in a 7% increase in system efficiency.

Cao et al. [32] performed a numerical study to assess the influence of incorporating phase change materials (PCM) into a solar chimney system, considering the climatic conditions of Hong Kong. The findings demonstrated that the integration of PCM led to a 14.8% increase in power generation compared to a conventional solar chimney. However, this enhancement

was accompanied by a 7.6% decrease in ventilation performance relative to a configuration combining the solar chimney with photovoltaic (PV) panels, indicating a performance trade-off between thermal storage and airflow efficiency. Esmail et al. [33] suggested three types of turbines were numerical analysis to study on the performance of SCPP. The conventional blade element theory (BET), a modified BET, and the matrix through flow method (MTFM) are the three turbine designs that are taken into consideration. The results demonstrated that the BET's updated version produced the most power. Kebabsa et al. [34] introduced a novel solar chimney tower design, revealing that thermal efficiency is highly influenced by variations in both external and internal tower radii (ETR and ITR). The new design achieved a 32% increase in power output, while reducing the tower surface area by 40%, with only a minimal power drop of 6.06%.

Alkaragoly et al. [35] proposed a hybrid SC–PV–EAHE system to improve ventilation, thermal comfort, and electricity generation. Simulations using summer data from Baghdad and Tehran showed it met cooling demands (116–1500 W), while 16 PV panels generated up to 1042 W in Tehran and 768 W in Baghdad, covering most residential energy needs. El Hadji et al. [36] conducted an experiment investigation the effect of solar radiation concentration on a solar chimney collector (SCCC), with a (2 m × 2 m × 2 m) test building in Dakar. Results showed that adding three reflectors significantly increased solar radiation absorption, which findings confirm that radiation concentration enhances chimney performance, promoting improved natural ventilation in bioclimatic buildings. Esmail et al. [37] conducted an experimental investigation to examine the impact of wind speed on the airflow characteristics within the chimney of a SCPP. Key parameters monitored during the experiment included solar radiation, ambient temperature, wind speed above the chimney, and the internal air velocity. The results revealed that an increase in wind speed at the chimney outlet significantly increased the updraft air velocity, which improved the SCPP's overall effectiveness and performance. Mahmood and Aljubury [38] tested an original hybrid PV/evaporative cooling (PV/EC) system to enhance PV efficiency and provide cool air. The system integrates cooling pads beneath the PV panel, reducing roof heat gain. Using pads of varying thicknesses, efficiency improved by up to 11.2%, with panel cooling reaching 20°C and air supplied at 24.7°C and 71% RH. Results confirm improved thermal and electrical performance. Sundararaj et al. [39] optimized a solar chimney power plant with a semi-convergent collector and divergent chimney using CFD and experiments. Results showed a temperature rise of 18 K and increased mass flow from 0.04 to 0.06 kg/s, enhancing power output. Simulation closely matched experiments, supporting the design's potential for large-scale green energy generation. Hassan [40] modified power plant of solar chimney incorporated with a mechanism for cooling via solid sorption is proposed to improve solar energy utilization and power output. The main modification consists of positioning the condenser tubes at the collector inlet, enabling the incoming airflow to absorb heat from the condenser before entering the system. A dynamic model was developed to assess performance. The main finding shows a 5.95% enhanced in output power and a 6% boost in solar-to-electricity efficiency liken to the original design, confirming the benefits of heat recovery from condensation.

Elsayed et al. [41] evaluated a hybrid energy system combining a small-scale solar chimney with bladeless and

horizontal-axis wind turbines (VBSCS) for sustainable power generation in Egypt. Using modeling, CFD, and experiments, the impact of absorber materials was assessed. Shredded rubber improved thermal performance, increasing output to 0.25 W compared to 0.18 W for concrete. The VBSCS achieved 0.29 W, showing a 61.1% improvement over the basic system. Results confirm that design and material choices significantly affect system efficiency. Merie and Ahmed [42] examined how cloudy weather affects PV/solar chimney performance. Tests on clear and cloudy days showed power output dropped from 341.92 W to 187.88 W, and total efficiency fell from 69.65% to 54.12% at noon. The results confirm high sensitivity to reduced solar irradiance. Nie et al. [43] suggested a solar chimney designed for greenhouse structures that has a rectangular collector to promote agricultural and clean energy. By adjusting the infusion angle to minimize resistance loss as determined by a transition factor, collector efficiency is greatly increased. The optimal design, which was based on response surface approach, achieved 48.75% efficiency and (-6.1 Pa) static pressure, which is a 213% and 563% increase over the original model, respectively.

Abo-Zahhad et al. [44] examined the impact of ground thermal properties on SCPP performance. Simulations, validated with the Manzanares prototype, showed that improved conductivity and specific heat enhanced efficiency. Under Aswan's climate, efficiency reached 39.11%, with a 17.71% power gain, highlighting the value of optimizing ground materials. Ba-swaimi et al. [45] assessed integrated hybrid renewable energy systems (IHRES) for healthcare using HOMER Pro. The optimal standalone PV/BES/Genset setup cut costs by 76.81% with 95.2% renewable energy. Grid-connected PV/BES/Grid achieved the lowest levelized cost of energy (LCOE) (\$0.0879/kWh) and 91.2% REF, showing grid integration boosts reliability and sustainability. Qasim et al. [46] evaluated hybrid power systems for remote Iraqi communities using HOMER Pro. The optimal PV/WT/BESS/DG setup produced 90.1 MWh/year, with 71.7% from solar, 27.8% from wind, and minimal diesel use. It achieved a low LCOE of \$0.0521/kWh, the net present cost (NPC) of \$40,681, and CO₂ emissions of 426 kg/year, a major reduction compared to diesel-heavy systems. The study offers a scalable, cost-effective, and sustainable energy solution for off-grid regions in Iraq.

Based on the above, there is a great opportunity to invest in solar energy and convert it into sustainable energy in the process of reducing fossil fuel consumption by incorporating it into architectural designs during the construction of public buildings, especially when heating and ventilation within the interior space.

This study highlights the critical influence of chimney geometry and airflow dynamics on the performance of HSC systems, emphasizing that design modifications such as wall slopes and entrance height can significantly affect efficiency. Building upon a validated baseline model from previous research [26]. Three geometric configurations were proposed to enhance energy production: the first incorporating four internal nozzles, the second adding a canopy at the chimney outlet to stabilize and direct airflow, and the third combining both features in an integrated nozzle-canopy design. Using CFD simulations supported by prior experimental validation, the analysis examined airflow patterns, temperature distribution, and power generation across these configurations. The results demonstrate that structural interventions can

markedly improve system efficiency, with the combined nozzle-canopy model delivering the highest gains in airflow velocity and energy conversion. These findings offer practical insights into optimizing chimney geometry for HSC systems, supporting their application in sustainable building ventilation and decentralized renewable energy solutions.

2. RESEARCH METHODOLOGY

This research adopts a quantitative-numerical approach based on CFD modeling to analyze the performance of the HSC, incorporating experimental data from previous studies to validate the results. The research aims to: Evaluate the thermal and electrical efficiency of the hybrid chimney under different operating conditions for the three models. Identify the optimum factors for improving ventilation and power generation such as airflow velocity. Compare the performance with conventional power systems.

2.1 Describe the model geometry

Model A is to add internal four nozzles to a 6 m long chimney to take advantage of the air concentration in the middle of the chimney directed directly to the generator fan in four areas as shown in Figure 2. The B model is to add a canopy at the end of the chimney that redirects the lateral air upwards so that it does not form a barrier to the chimney nozzle, in addition to increasing the possibility of drawing air from above as a result of the lateral air movement. Model C is to combine Model A with Model B and then solve the cases shown in Figure 3.

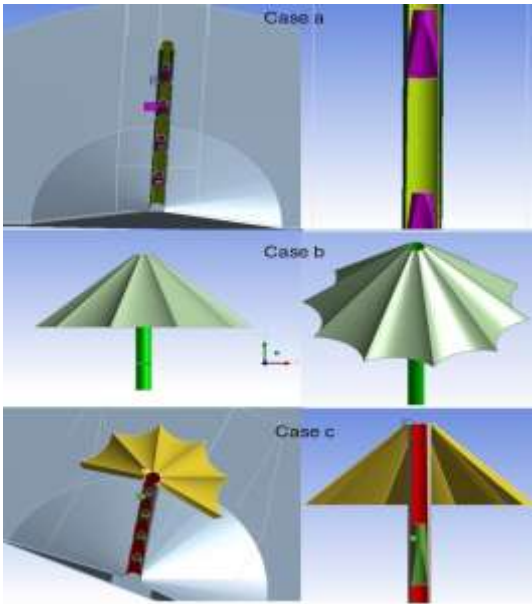


Figure 2. Overall design of the three models a, b, and c to improve and develop HSC

2.2 Mesh generation and independence check

A prototype was designed for the purpose of verifying the validity of the solution based on a previous study Figure 4 regarding the dimensions and materials used in the simulation as shown in Figure 3, which also shows the distribution of elements and nodes (mesh). Then the simulation was

conducted based on the data of the previous study in determining the materials used and determining the boundary condition [26]. After verifying the correctness of the solution and an acceptable error rate for the prototype, the other three designs were moved to modify the prototype while maintaining the physical properties and boundary condition. Table 1 represents the number of nodes and elements for the prototype and models a, b and c.

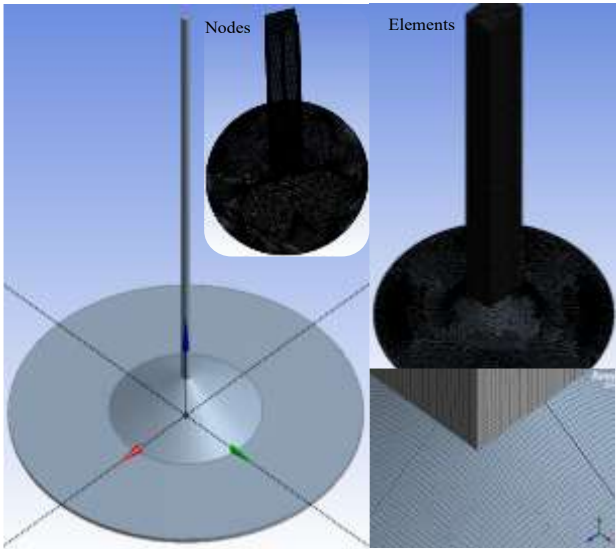


Figure 3. Prototype with elements and nodes

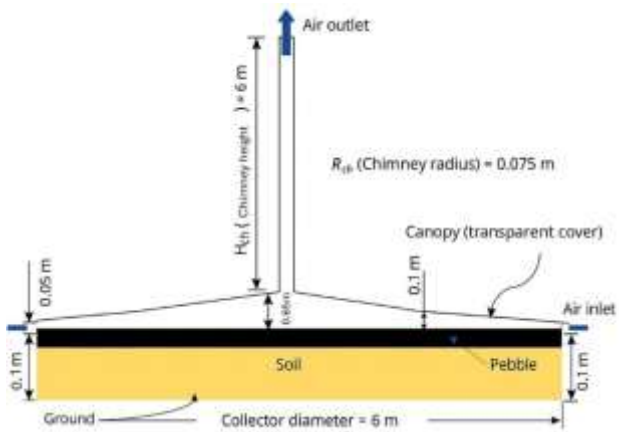
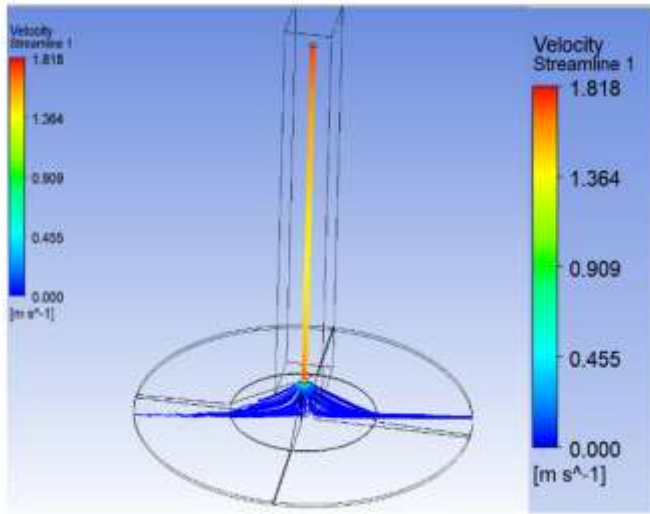


Figure 4. Diagram of the traditional SC computer model [26]

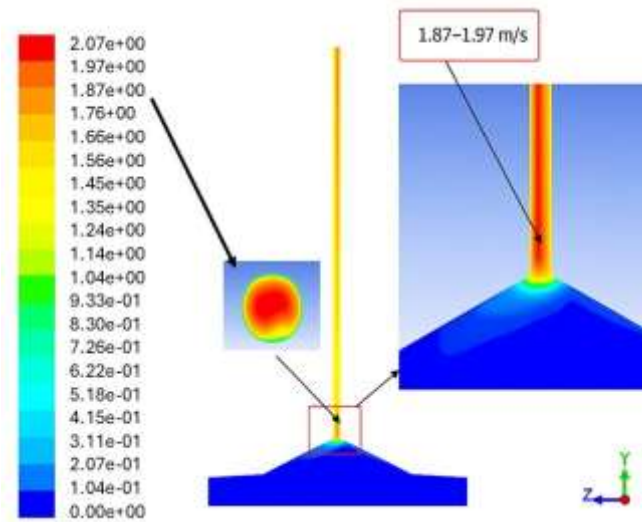
To verify the validity of the results, a model of previous studies was simulated and then compared with the results obtained, shown in Figure 5. The results in previous studies show that the speed in the first case is 1.97 m/s, while in the current study it is 1.818 m/s, with the absolute error is 7.7%. These ratios are considered acceptable. Both studies were simulated at standard atmospheric conditions.

Table 1. Distribution of elements and nodes for prototype

Model	Elements	Nodes	V_{max} (m/s)	Error (Velocity) %
Coarse	1231999	592866	1.746	11.370
Medium	1305370	603161	1.797	8.781
Fine	1400573	699133	1.813	7.969
More fine	1491099	735737	1.818	7.7



a) Current study (Prototype)



b) Al-Kayiem [26]

Figure 5. Validation of current study

2.3 Governing equations and models

The mass, momentum, and energy conservation equations governing the HSC's flow model were solved using commercial ANSYS Fluent after appropriate boundary conditions were applied. The steady-state version of the governing equations is as follows [47-51]:

Continuity equation:

$$\frac{\partial}{\partial x}(u) + \frac{\partial}{\partial y}(v) + \frac{\partial}{\partial z}(w) = 0 \quad (1)$$

X – direction (U momentum):

$$\rho \left(\frac{\partial}{\partial x}(uu) + \frac{\partial}{\partial y}(uv) + \frac{\partial}{\partial z}(uw) \right) = -\frac{\partial p}{\partial x} + \mu \left(\left(\frac{\partial^2 u}{\partial x^2} \right) + \left(\frac{\partial^2 u}{\partial y^2} \right) + \left(\frac{\partial^2 u}{\partial z^2} \right) \right) \quad (2)$$

Y – direction:

$$\rho \left(\frac{\partial}{\partial x}(uv) + \frac{\partial}{\partial y}(vv) + \frac{\partial}{\partial z}(vw) \right) = -\frac{\partial p}{\partial y} + \mu \left(\left(\frac{\partial^2 v}{\partial x^2} \right) + \left(\frac{\partial^2 v}{\partial y^2} \right) + \left(\frac{\partial^2 v}{\partial z^2} \right) \right) - g\rho \quad (3)$$

Z – direction:

$$\rho \left(\frac{\partial}{\partial x}(uw) + \frac{\partial}{\partial y}(vw) + \frac{\partial}{\partial z}(ww) \right) = -\frac{\partial p}{\partial z} + \mu \left(\left(\frac{\partial^2 w}{\partial x^2} \right) + \left(\frac{\partial^2 w}{\partial y^2} \right) + \left(\frac{\partial^2 w}{\partial z^2} \right) \right) \quad (4)$$

And energy conservation equation is:

$$C_p \rho \left(\frac{\partial}{\partial x}(uT) + \frac{\partial}{\partial y}(vT) + \frac{\partial}{\partial z}(wT) \right) = k \left(\left(\frac{\partial^2 T}{\partial x^2} \right) + \left(\frac{\partial^2 T}{\partial y^2} \right) + \left(\frac{\partial^2 T}{\partial z^2} \right) \right) + S_E \quad (5)$$

The modeled transport equations for k and ε in the realizable (k, ε) model are:

k – equation:

$$\rho \frac{\partial}{\partial x_j}(kU_j) = \frac{\partial}{\partial x_j} \left[\left(\mu + \frac{\mu_t}{\sigma_k} \right) \frac{\partial k}{\partial x_j} \right] + S_k \quad (6)$$

ε – equation:

$$\rho \frac{\partial}{\partial x_j}(\varepsilon U_j) = \frac{\partial}{\partial x_j} \left[\left(\mu + \frac{\mu_t}{\sigma_\varepsilon} \right) \frac{\partial \varepsilon}{\partial x_j} \right] + S_\varepsilon \quad (7)$$

where,

S_k : source of kinetic energy

S_ε : source of dissipation rate

The following formula was used to determine the density in the Boussinesq approximation:

$$\rho = \rho_0[1 - \beta(T - T_0)] \quad (8)$$

2.4 Boundary conditions

The CFD domain with the boundary condition for conventional and HSC listed in Table 2, and Figure 6 shows the air intake and outlet areas, where the blue arrow indicates the air intake area, while the red arrow indicates the air outlet area.

Table 2. Inlet and outlet conditions of conventional and hybrid for solar chimney models used in simulations

Region	Set	Rate
bottom	wall	Adiabatic
Canopy	wall	Hw = 8W/m ² .K
Chimney	wall	Adiabatic
Inlet of collector	Inlet	P _{gauge} = 0 T _{amb} = 307 K
Outlet of chimney	Outlet	P _{gauge} = 0 T _{amb} = 307 K

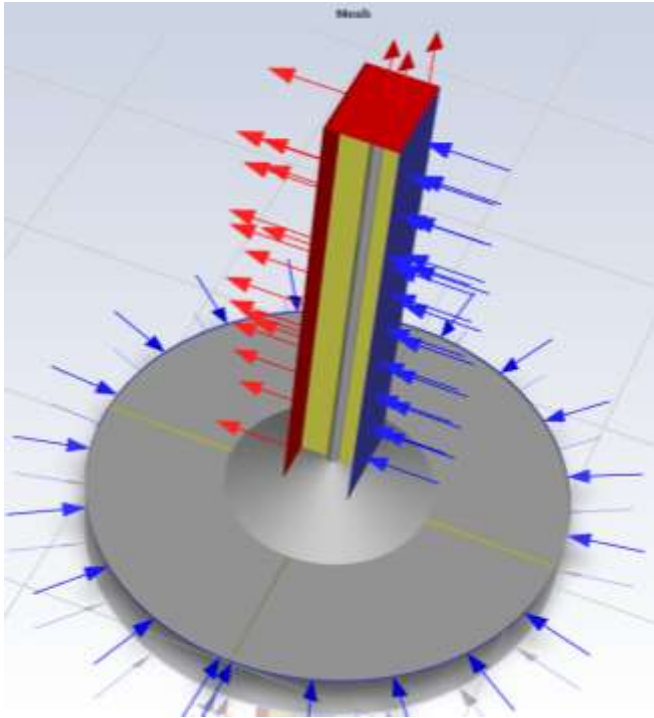


Figure 6. Air intake and exhaust locations

3. RESULTS AND DISCUSSION

After comparing the initial results of the proposed model with previous studies to verify the validity of the model and the accuracy of the data, simulations were conducted for the three proposed models to obtain and analyze the results. The simulation results of the three models for flow velocity were different as shown in the three figures below, see Figures 7-9.

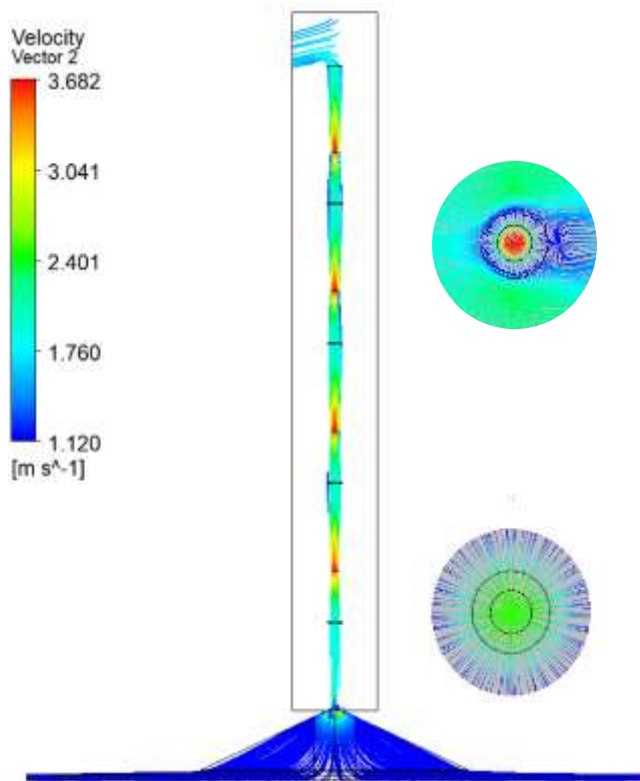


Figure 7. Velocity field for model A

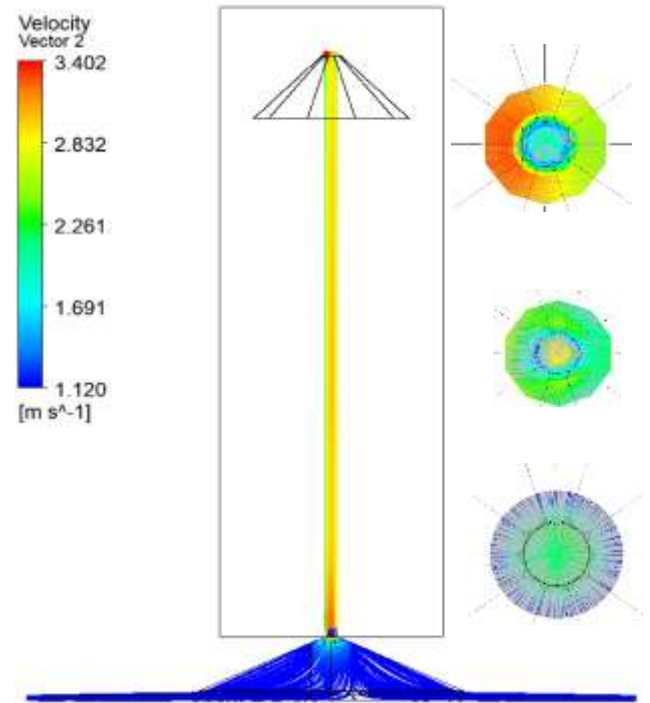


Figure 8. Velocity field for model B

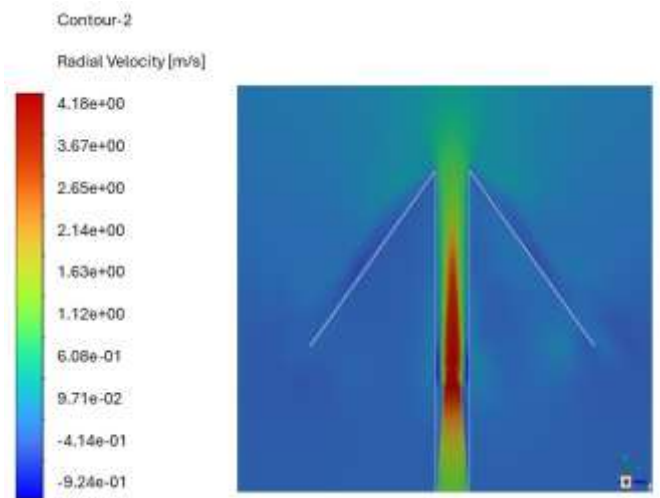


Figure 9. Velocity field for model C

3.1 Velocity field distribution

Figure 7 illustrates the vertical and radial velocity vector distributions within the solar chimney system incorporating a converging nozzle structure. The primary aim of the nozzle is to enhance airflow acceleration by narrowing the flow path and thereby increasing the vertical momentum of the rising heated air.

The vertical velocity contours reveal that the airflow is effectively accelerated through the nozzle throat, achieving a maximum velocity of approximately 3.68 m/s near the chimney axis. The high-velocity jet formation is distinctly visible along the chimney centerline, indicating that the internal nozzle significantly improves the thermal-to-kinetic energy conversion. This effect is consistent with classical nozzle theory, where reduced cross-sectional area leads to increased flow speed under buoyancy-driven pressure gradients.

The streamlines at the chimney entrance show a smooth and directed flow convergence from the collector region toward the nozzle, confirming efficient flow guidance and minimal recirculation losses. The canopy effect appears to complement the nozzle function by aiding in radial flow collection and channeling it upward. This combination results in a stable vertical jet, which is crucial for maximizing the performance of turbines positioned at the chimney base or mid-height.

Cross-sectional velocity vector maps further highlight the symmetry and consistency of the flow within the chimney. The central core maintains high upward momentum, while the surrounding flow regions exhibit well-distributed radial and tangential velocities, contributing to the overall flow stability. The vortex structures observed in the radial slices suggest the presence of shear layer development, which could enhance turbulent mixing and improve energy extraction if strategically harnessed.

Figure 8 presents the vertical and cross-sectional velocity vector distributions for the solar chimney system featuring an internal canopy structure located in the upper chimney region. The canopy, arranged in a pyramidal or conical configuration, serves to influence the internal airflow dynamics, particularly by shaping the updraft near the chimney outlet.

The velocity vector distribution shows a highly concentrated vertical jet along the chimney centerline, reaching a maximum axial velocity of approximately 3.40 m/s. This strong central updraft indicates the effective funneling effect created by the canopy, which confines the rising heated air and promotes axial flow stability, which increases the velocity about (45%) if compared with previous study [26].

From the streamline patterns at the base and collector entrance, it is evident that air is efficiently guided into the chimney, with minimal flow separation. The internal canopy helps reduce velocity dispersion near the chimney top by maintaining flow alignment along the vertical axis, thus minimizing losses due to radial expansion.

The cross-sectional velocity vector plots further support this observation. The canopy-induced confinement creates a well-defined and symmetrical velocity distribution, with reduced swirl and limited lateral velocity components. The uppermost radial slice, taken near the canopy region, shows a pressure equalization effect, where the flow becomes more uniform as it approaches the exit. This behavior is beneficial for turbine installations at the chimney outlet, where a steady and directed velocity field enhances mechanical efficiency and reduces mechanical stress on turbine blades. The nozzle modification generates elevated turbulent kinetic energy (TKE) downstream of the throat due to strong shear layers, which enhances thermal to kinetic energy conversion but also introduces localized dissipation and unsteady flow features. In contrast, the canopy reduces turbulence intensity at the outlet by directing the updraft vertically, thereby suppressing large-scale vortex shedding and improving flow coherence. When both modifications are combined, the accelerated jet produced by the nozzle is stabilized by the canopy, yielding a concentrated high-velocity core with minimized lateral swirl. Vortex structures in this integrated configuration are confined to smaller, less energetic eddies, reducing pressure fluctuations and turbulence-driven energy losses while sustaining the highest power output. This analysis indicates that while the nozzle favors acceleration and the canopy favors stabilization, their combination provides the most effective balance, enhancing aerodynamic efficiency and reducing flow instabilities.

Moreover, the canopy acts as a flow stabilizer, preventing excessive turbulence and vortex formation at the exit, which are typically detrimental to energy conversion efficiency. The mild shear zones observed around the canopy base suggest limited energy dissipation, indicating that the structure aids in preserving the vertical kinetic energy of the rising air column.

Figure 9 presents the radial velocity contours inside the solar chimney system with an integrated nozzle and canopy. The results demonstrate the substantial impact of these design modifications on the internal flow field and overall performance.

The simulation reveals a prominent increase in radial velocity along the central axis of the chimney, particularly downstream of the nozzle. The maximum recorded radial velocity reached approximately 4.18 m/s, indicating a strong acceleration effect due to the converging nozzle geometry. This accelerated core flow confirms the effectiveness of the nozzle in enhancing the chimney's draft effect by converting thermal buoyancy into kinetic energy more efficiently which increases the velocity about (55.2%) If compared with previous study [26].

In addition, the angled canopy structure positioned within the upper region of the collector redirects the incoming airflow toward the centerline of the chimney. This redirection contributes to the formation of a compressed central jet, improving the radial velocity gradient and creating a stronger updraft. The flow profile shows a clear distinction between the high-velocity core and the surrounding low-speed zones, suggesting the development of shear layers and enhanced turbulent mixing.

3.2 Temperature distribution analysis

Figure 10 displays the temperature contour within the solar chimney system equipped with an internal nozzle. The temperature distribution illustrates a clear thermal gradient from the collector base to the chimney outlet, with temperatures ranging from 298 K to 310 K. The highest temperatures are concentrated near the ground-level collector, where solar heating is most effective.

As air rises through the chimney, a gradual temperature drop is observed, confirming the conversion of thermal energy into kinetic energy. The nozzle contributes to this process by accelerating the heated air, which enhances the chimney's buoyancy-driven flow. The relatively uniform vertical temperature distribution within the chimney core indicates stable upward motion and efficient energy transfer.

Figure 11 shows the temperature distribution within the solar chimney system incorporating an internal canopy. The temperature gradient ranges from 298 K at the base to a maximum of 310 K near the chimney centerline. The highest temperature region is concentrated along the vertical axis, indicating efficient solar heating and sustained buoyancy-driven flow.

The presence of the canopy helps to confine and direct the heated air upward, resulting in a more focused and continuous thermal column. This confinement minimizes radial heat dispersion, enhancing thermal energy retention along the centreline. The smooth temperature transition from the collector to the outlet suggests stable thermal stratification, which is essential for maintaining a steady updraft.

Figure 12 presents the temperature contours of the solar chimney system integrating both an internal nozzle and canopy. The combined configuration shows a well-defined

and continuous high-temperature core, with peak values reaching approximately 310.8 K. The heated air is effectively guided along the chimney axis, with minimal radial dispersion.

The nozzle at the base enhances thermal energy conversion by accelerating the incoming heated air, while the canopy at the top confines and stabilizes the vertical flow. This synergy creates a uniform thermal plume that extends from the collector to the chimney outlet. The outer temperature gradient indicates effective thermal insulation and containment within the core flow.

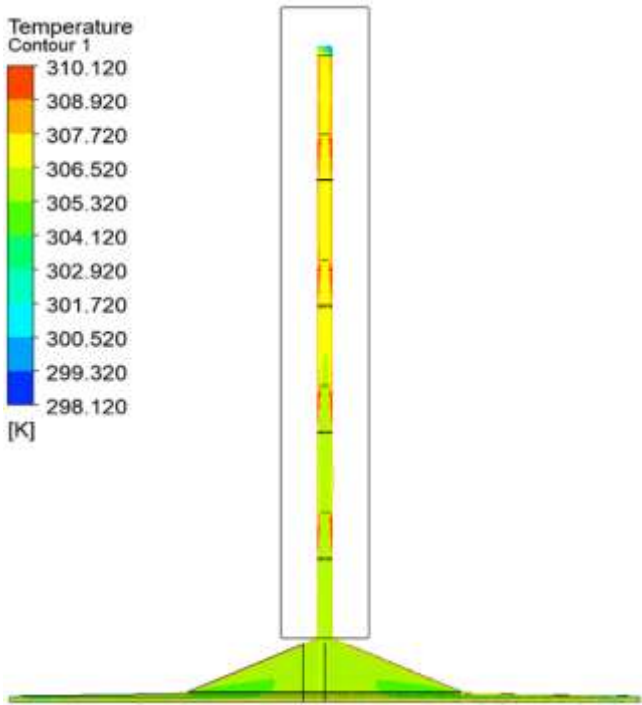


Figure 10. Temperature contour model A

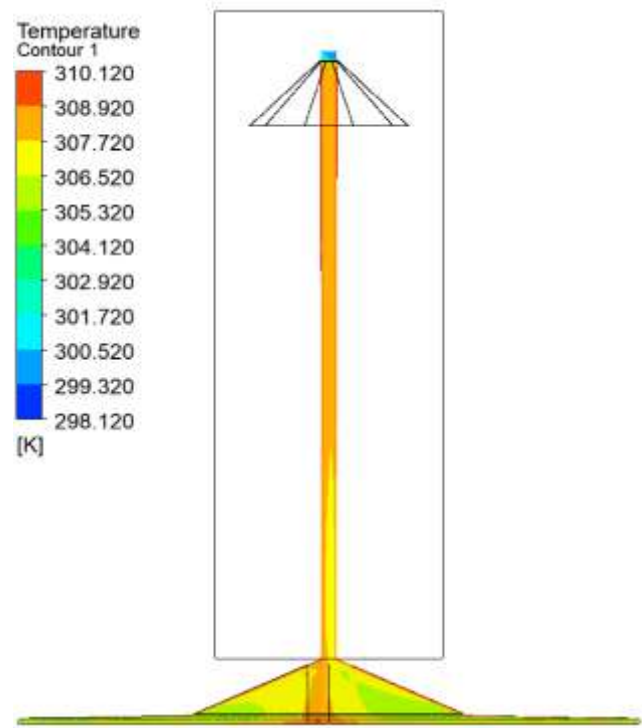


Figure 11. Temperature contour model B

Temperature distribution under the canopy shows slight cooling near the edges, suggesting efficient heat extraction at the center, where the turbine can be most effectively positioned. The combined effect of both components improves thermal stratification, increases buoyancy force, and ensures enhanced vertical draft.

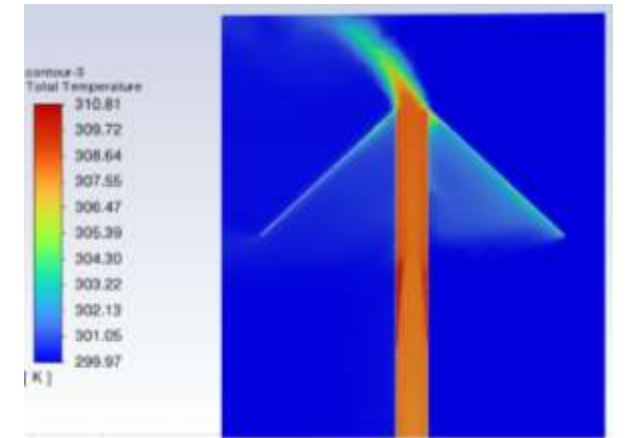
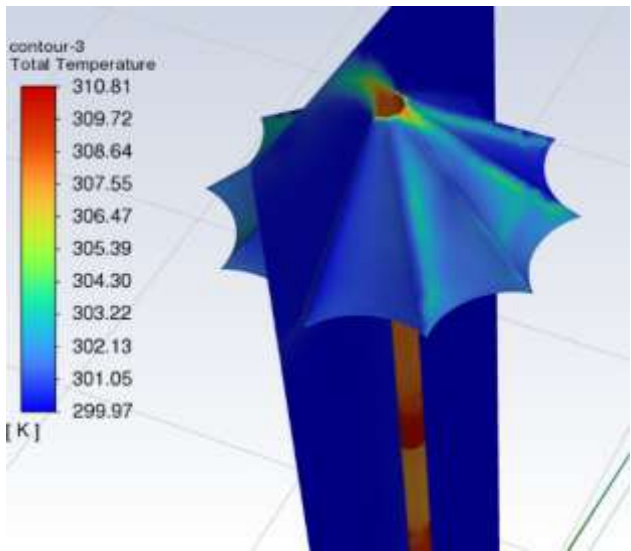
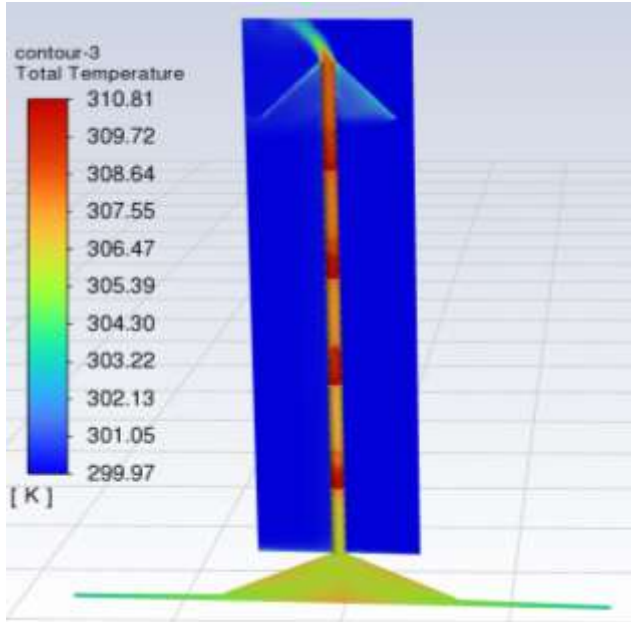


Figure 12. Temperature contour model C

3.3 Power production estimate

The properties of the air inside the vortex generator are covered in this section. For the vortex domain (from the base of the chimney to the outer region), area-weighted average data are shown in the form of graphs and outlines.

Theoretically, Table 3 uses the following formula to calculate the kinetic power produced by the solar chimney, which is based on the mass flow rate of the air entering the chimney [32]:

$$P_{out} = \frac{1}{2} \rho A_{base\ chimney} V_{out}^3 \quad (9)$$

Figure 13 shows the direct relationship between airflow velocity and power production in the HSC. The baseline case produced only 0.81×10^{-1} W at a velocity of 1.97 m/s, while the nozzle modification (Model A) increased velocity to 3.628 m/s and boosted power to 5.06×10^{-1} W (84% gain). The canopy (Model B) achieved 3.402 m/s and 4.17×10^{-1} W (77.6% gain). The combined nozzle-canopy design (Model C) delivered the best performance, with 4.18 m/s velocity and 7.74×10^{-1} W power output (80.6% improvement). The figure highlights that higher velocities, particularly from the integrated design, significantly enhance energy generation efficiency.

Table 3. Estimated power production of three models

Cases	Velocity (m/s)	Power Production $\times 10^{-1}$ (W)	Power in %
Previous study	1.970	0.810	-
Model A	3.628	5.06	84.0 %
Model B	3.402	4.17	77.6 %
Model C	4.18	7.74	80.6 %

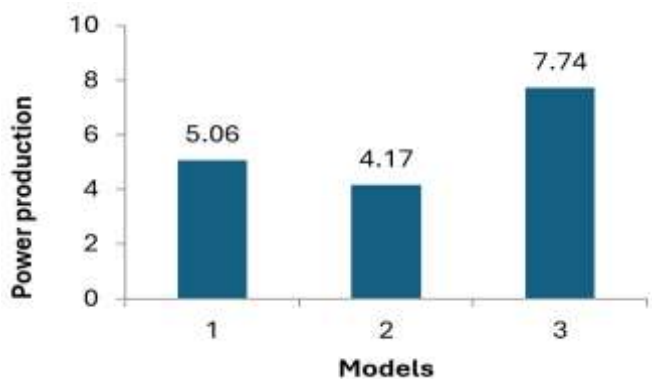


Figure 13. The impact of flow velocity on power production

3.4 The trade-off between structural complexity and performance gain

The results demonstrated that geometric interventions directly influence updraft intensity and energy conversion efficiency. Specifically, the nozzle improved internal airflow speed by constricting and directing the thermal plume, while the canopy reduced exit turbulence and enhanced vertical flow coherence. The combined nozzle-canopy design produced the most favorable outcomes, achieving a substantial increase in air velocity and power potential.

Despite these performance improvements, a trade-off arises

between structural complexity and practical applicability. Incorporating internal nozzles requires precise fabrication and alignment to ensure smooth flow convergence, while canopy structures add to construction demands, material usage, and long-term maintenance requirements. When both modifications are integrated, the overall complexity increases further, potentially elevating system cost and reducing ease of deployment in resource-limited regions. Additionally, highly complex geometries may compromise system robustness under fluctuating environmental conditions.

Therefore, while even minor structural changes can yield significant performance gains, practical applications must balance efficiency improvements with construction feasibility, cost-effectiveness, and operational sustainability. These insights confirm the critical role of passive design optimization in solar-driven ventilation systems, especially in hot-climate regions where such strategies support sustainable building integration and renewable energy utilization.

4. CONCLUSIONS

The geometric modifications applied to the HSC demonstrated distinct mechanisms for improving flow and thermal performance. The nozzle modification accelerated the updraft by narrowing the flow passage, which increased the axial velocity to approximately 3.68 m/s, representing an 84% improvement compared with the baseline case (1.97 m/s). This acceleration enhanced the conversion of thermal energy into kinetic energy, as confirmed by the more uniform vertical temperature gradient observed within the chimney core. The canopy modification, in contrast, contributed mainly to flow stabilization, directing lateral airflow upward and reducing turbulence at the outlet. This resulted in a maximum axial velocity of about 3.40 m/s, which corresponds to a 45% improvement over the baseline, while thermally it minimized radial heat dispersion and maintained buoyancy-driven stratification along the chimney axis. The integration of both features in the nozzle-canopy design provided a synergistic effect, combining acceleration with stabilization, and produced the highest performance. The maximum velocity reached 4.18 m/s, equating to a 55% increase over the reference study, while the corresponding power production rose to 7.74×10^{-1} W, reflecting an 80.6% gain compared with the conventional configuration. This demonstrates that while each modification has a specific contribution—nozzle for acceleration and canopy for stabilization, their combined effect offers the most effective enhancement in both aerodynamic and thermal performance. Future research should focus on simplified yet effective design variants, supported by experimental validation and parametric optimization, to ensure the scalability of HSCs in zero-energy buildings and decentralized renewable power systems.

ACKNOWLEDGEMENTS

The authors would like to express their sincere gratitude to the Kufa Center for Advanced Simulation in Engineering (KCASE), Faculty of Engineering, University of Kufa, for providing access to its advanced computing facilities, which greatly contributed to the engineering analysis conducted in this study.

REFERENCES

- [1] International Energy Agency. (2025). National climate resilience assessment for Iraq. National Climate Resilience Assessments. IEA, Paris. <https://www.iea.org/reports/national-climate-resilience-assessment-for-iraq>.
- [2] Fereidoni, S., Fereidooni, L., Shabestari, S.T., Esmaeili, M.S., Zare, M., Kasaeian, A. (2025). Application of solar chimneys and hybrid solar chimneys for ventilation in buildings: A review. *Solar Energy*, 288: 113246. <https://doi.org/10.1016/j.solener.2025.113246>
- [3] Sebestyén, V. (2021). Renewable and sustainable energy reviews: Environmental impact networks of renewable energy power plants. *Renewable and Sustainable Energy Reviews*, 151: 111626. <https://doi.org/10.1016/j.rser.2021.111626>
- [4] Soltani, A., Imani, M.A. (2024). Overcoming implementation barriers to renewable energy in developing nations: A case study of Iran using MCDM techniques and Monte Carlo simulation. *Results in Engineering*, 24: 103213. <https://doi.org/10.1016/j.rineng.2024.103213>
- [5] Ghafar, H., Yusoff, H., Nasir, S.M.F.S.A., Abd Ghani, K.D., Ismail, M.A. (2025). Performance evaluation of natural and forced convection in solar dryers for mullet fish. *Jurnal Teknologi (Sciences & Engineering)*, 87(1): 43-52. <https://doi.org/10.11113/jurnalteknologi.v87.22448>
- [6] Jasim, Q.K., Kanbar, M.W., Saleh, N.M. (2022). Photovoltaic solar chimney system: A review. *Journal of Global Scientific Research in Mechanical and Materials Engineering*, 7(6): 2358-2396. <https://doi.org/10.5281/zenodo.6633552>
- [7] Saleh, M.J., Atallah, F.S., Algburi, S., Ahmed, O.K. (2023). Enhancement methods of the performance of a solar chimney power plant. *Results in Engineering*, 19: 101375. <https://doi.org/10.1016/j.rineng.2023.101375>
- [8] Ahmed, O.K., Algburi, S., Ali, Z.H., Ahmed, A.K., Shubat, H.N. (2022). Hybrid solar chimneys: A comprehensive review. *Energy Reports*, 8: 438-460. <https://doi.org/10.1016/j.egyr.2021.12.007>
- [9] Rtemi, L.A., El-Osta, W., Attaiep, A. (2023). Hybrid system modeling for renewable energy sources. *Journal of Solar Energy and Sustainable Development*, 12(1).
- [10] Yusop, A.M., Alzari, A., Zakaria, M.H., Jahari, A.N.M., Sulaiman, N.A., Khamil, K.N., Mohammed, R., Sultan, J.M. (2024). Thermal application using pyramid solar still to enhance the producing of clean water. *Jurnal Teknologi (Sciences & Engineering)*, 86(5): 59-67. <https://doi.org/10.11113/jurnalteknologi.v86.20935>
- [11] National Academies. (n.d.). Net-zero emissions by 2050. <https://nap.nationalacademies.org/resource/other/dels/net-zero-emissions-by-2050>.
- [12] Aljashaami, B.A., Ali, B.M., Salih, S.A., Alwan, N.T., Majeed, M.H., Ali, O.M., Alomar, O.R., Velkin, V.I., Shcheklein, S.E. (2024). Recent improvements to heating, ventilation, and cooling technologies for buildings based on renewable energy to achieve zero-energy buildings: A systematic review. *Results in Engineering*, 23: 102769. <https://doi.org/10.1016/j.rineng.2024.102769>
- [13] US Energy Information Administration. (2021). EIA projects nearly 50% increase in world energy use by 2050, Led by Growth in Renewables. <https://www.eia.gov/todayinenergy/detail.php?id=49876>.
- [14] Olabi, A.G., Elsaid, K., Obaideen, K., Abdelkareem, M.A., Rezk, H., Wilberforce, T., Maghrabie, H.M., Sayed, E.T. (2023). Renewable energy systems: Comparisons, challenges and barriers, sustainability indicators, and the contribution to UN sustainable development goals. *International Journal of Thermofluids*, 20: 100498. <https://doi.org/10.1016/j.ijft.2023.100498>
- [15] Ukoba, K., Yoro, K.O., Eterigho-Ikelegbe, O., Ibegbulam, C., Jen, T.C. (2024). Adaptation of solar power in the global south: Prospects, challenges and opportunities. *Heliyon*. <https://doi.org/10.1016/j.heliyon.2024.e28009>
- [16] Salim, H.K., Stewart, R.A., Sahin, O., Dudley, M. (2019). Drivers, barriers and enablers to end-of-life management of solar photovoltaic and battery energy storage systems: A systematic literature review. *Journal of Cleaner Production*, 211: 537-554. <https://doi.org/10.1016/j.jclepro.2018.11.229>
- [17] Zhang, Y., Sivakumar, M., Yang, S., Enever, K., Ramezaniapour, M. (2018). Application of solar energy in water treatment processes: A review. *Desalination*, 428: 116-145. <https://doi.org/10.1016/j.desal.2017.11.020>
- [18] Winter, N. (2022). Renewables 2022 global status report: United states of America factsheet. REN21. France. <https://coilink.org/20.500.12592/67p8v5>.
- [19] International Renewable Energy Agency. (2025). Renewable capacity statistics 2025. International Renewable Energy Agency, Abu Dhabi. <https://www.irena.org/Publications/2025/Mar/Renewable-capacity-statistics-2025>.
- [20] Bamisile, O., Acen, C., Cai, D., Huang, Q., Staffell, I. (2025). The environmental factors affecting solar photovoltaic output. *Renewable and Sustainable Energy Reviews*, 208: 115073. <https://doi.org/10.1016/j.rser.2024.115073>
- [21] Kabir, E., Kumar, P., Kumar, S., Adelodun, A.A., Kim, K.H. (2018). Solar energy: Potential and future prospects. *Renewable and Sustainable Energy Reviews*, 82: 894-900. <https://doi.org/10.1016/j.rser.2017.09.094>
- [22] Bansal, N.K., Mathur, R., Bhandari, M.S. (1993). Solar chimney for enhanced stack ventilation. *Building and Environment*, 28(3): 373-377. [https://doi.org/10.1016/0360-1323\(93\)90042-2](https://doi.org/10.1016/0360-1323(93)90042-2)
- [23] Hassan, Q., Algburi, S., Sameen, A.Z., Salman, H.M., Jaszczur, M. (2023). A review of hybrid renewable energy systems: Solar and wind-powered solutions: Challenges, opportunities, and policy implications. *Results in Engineering*, 20: 101621. <https://doi.org/10.1016/j.rineng.2023.101621>
- [24] Ghorbani, B., Ghashami, M., Ashjaee, M., Hosseinzadegan, H. (2015). Electricity production with low grade heat in thermal power plants by design improvement of a hybrid dry cooling tower and a solar chimney concept. *Energy Conversion and Management*, 94: 1-11. <https://doi.org/10.1016/j.enconman.2015.01.044>
- [25] Zou, Z., He, S. (2015). Modeling and characteristics analysis of hybrid cooling-tower-solar-chimney system. *Energy Conversion and Management*, 95: 59-68. <https://doi.org/10.1016/j.enconman.2015.01.085>

- [26] Al-Kayiem, H.H., Aurybi, M.A., Gilani, S.I., Ismaeel, A.A., Mohammad, S.T. (2019). Performance evaluation of hybrid solar chimney for uninterrupted power generation. *Energy*, 166: 490-505. <https://doi.org/10.1016/j.energy.2018.10.115>
- [27] Hou, Y., Li, H., Li, A. (2019). Experimental and theoretical study of solar chimneys in buildings with uniform wall heat flux. *Solar Energy*, 193: 244-252. <https://doi.org/10.1016/j.solener.2019.09.061>
- [28] Abdelsalam, E., Kafiah, F., Tawalbeh, M., Almomani, F., Azzam, A., Alzoubi, I., Alkasrawi, M. (2021). Performance analysis of hybrid solar chimney-power plant for power production and seawater desalination: A sustainable approach. *International Journal of Energy Research*, 45(12): 17327-17341. <https://doi.org/10.1002/er.6004>
- [29] Nugroho, A.M., Ahmad, M.H. (2014). Passive cooling performance of a solar chimney and vertical landscape applications in Indonesian terraced house. *Jurnal Teknologi (Sciences & Engineering)*, 70(7). <https://doi.org/10.11113/jt.v70.3585>
- [30] Moosavi, L., Zandi, M., Bidi, M., Behroozizade, E., Kazemi, I. (2020). New design for solar chimney with integrated windcatcher for space cooling and ventilation. *Building and Environment*, 181: 106785. <https://doi.org/10.1016/j.buildenv.2020.106785>
- [31] Singh, A.P., Kumar, A., Singh, O.P. (2020). Performance enhancement strategies of a hybrid solar chimney power plant integrated with photovoltaic panel. *Energy Conversion and Management*, 218: 113020. <https://doi.org/10.1016/j.enconman.2020.113020>
- [32] Cao, Y., Pourhedayat, S., Dizaji, H.S., Wae-Hayee, M. (2021). A comprehensive optimization of phase change material in hybrid application with solar chimney and photovoltaic panel for simultaneous power production and air ventilation. *Building and Environment*, 197: 107833. <https://doi.org/10.1016/j.buildenv.2021.107833>
- [33] Esmail, M.F.C., A-Elmagid, W.M., Mekhail, T., Al-Helal, I.M., Shady, M.R. (2021). A numerical comparative study of axial flow turbines for solar chimney power plant. *Case Studies in Thermal Engineering*, 26: 101046. <https://doi.org/10.1016/j.csite.2021.101046>
- [34] Kebabsa, H., Lounici, M.S., Daimallah, A. (2021). Numerical investigation of a novel tower solar chimney concept. *Energy*, 214: 119048. <https://doi.org/10.1016/j.energy.2020.119048>
- [35] Alkaragoly, M., Maerefat, M., Targhi, M.Z., Abdjlalel, A. (2022). An innovative hybrid system consists of a photovoltaic solar chimney and an earth-air heat exchanger for thermal comfort in buildings. *Case Studies in Thermal Engineering*, 40: 102546. <https://doi.org/10.1016/j.csite.2022.102546>
- [36] El Hadji, I.C., Thiam, A., Ndiogou, B.A., Azilinson, D., Sambou, V. (2022). Experimental investigation of solar chimney with concentrated collector (SCCC). *Case Studies in Thermal Engineering*, 35: 101965. <https://doi.org/10.1016/j.csite.2022.101965>
- [37] Esmail, M.F.C., Khodary, A., Mekhail, T., Hares, E. (2022). Effect of wind speed over the chimney on the updraft velocity of a solar chimney power plant: An experimental study. *Case Studies in Thermal Engineering*, 37: 102265. <https://doi.org/10.1016/j.csite.2022.102265>
- [38] Mahmood, D.M.N., Aljubury, I.M.A. (2022). Experimental investigation of a hybrid photovoltaic evaporative cooling (PV/EC) system performance under arid conditions. *Results in Engineering*, 15: 100618. <https://doi.org/10.1016/j.rineng.2022.100618>
- [39] Sundararaj, M., Rajamurugu, N., Anbarasi, J., Yaknesh, S., Sathyamurthy, R. (2022). Parametric optimization of novel solar chimney power plant using response surface methodology. *Results in Engineering*, 16: 100633. <https://doi.org/10.1016/j.rineng.2022.100633>
- [40] Hassan, H.Z. (2024). Performance enhancement of the basic solar chimney power plant integrated with an adsorption cooling system with heat recovery from the condenser. *Energies*, 17(1): 136. <https://doi.org/10.3390/en17010136>
- [41] Elsayed, A.M., Gaheen, O.A., Abdelrahman, M.A., Aziz, M.A. (2024). An experimental investigation of a solar chimney integrated with a bladeless wind turbine for sustainable energy harvesting. *Energy*, 304: 132154. <https://doi.org/10.1016/j.energy.2024.132154>
- [42] Merie, F.H., Ahmed, O.K. (2024). Experimental assessment of the performance of the PV/solar chimney under the cloudy weather. *Results in Engineering*, 23: 102605. <https://doi.org/10.1016/j.rineng.2024.102605>
- [43] Nie, J., Xu, J., Su, H., Gao, H., Jia, J., Guo, T. (2024). Optimization of characteristic parameters of rectangular solar chimney adapted to agricultural greenhouses. *Case Studies in Thermal Engineering*, 54: 103971. <https://doi.org/10.1016/j.csite.2024.103971>
- [44] Abo-Zahhad, E.M., Hachicha, A.A., Mistarihi, M.Z., Salim, M.H., Esmail, M.F. (2025). Optimization of ground material properties for enhanced solar chimney power plant efficiency: A CFD and RSM approach. *Energy Reports*, 13: 3929-3945. <https://doi.org/10.1016/j.egyr.2025.03.035>
- [45] Ba-swaimi, S., Verayiah, R., Ramachandramurthy, V.K., ALAhmad, A.K., Padmanaban, S. (2025). Optimal configuration and sizing of integrated hybrid renewable energy systems for sustainable power supply in healthcare buildings. *Results in Engineering*, 26: 104800. <https://doi.org/10.1016/j.rineng.2025.104800>
- [46] Qasim, M.A., Yaqoob, S.J., Bajaj, M., Blazek, V., Obed, A.A. (2025). Techno-economic optimization of hybrid power systems for sustainable energy in remote communities of Iraq. *Results in Engineering*, 25: 104283. <https://doi.org/10.1016/j.rineng.2025.104283>
- [47] Mohamad, B., Karoly, J., Zelentsov, A. (2020). CFD modelling of formula student car intake system. *Facta Universitatis, Series: Mechanical Engineering*, 18(1): 153-163. <https://doi.org/10.22190/FUME190509032M>
- [48] Nag, A., Dixit, A.R., Petru, J., Váňová, P., Konečná, K., Hloch, S. (2024). Maximization of wear rates through effective configuration of standoff distance and hydraulic parameters in ultrasonic pulsating waterjet. *Facta Universitatis, Series: Mechanical Engineering*, 21(2): 165-186. <https://doi.org/10.22190/FUME220523045N>
- [49] Qader, F.F., Mohamad, B., Hussein, A.M., Danook, S.H. (2024). Numerical study of heat transfer in circular pipe filled with porous medium. *Pollack Periodica*, 19(1): 137-142. <https://doi.org/10.1556/606.2023.00869>
- [50] Miri, R., Mliki, B., Mohamad, B.A., Abbassi, M.A., Oreijah, M., Guedri, K., Abderafi, S. (2023). Entropy generation and heat transfer rate for MHD forced convection of nanoliquid in presence of viscous

- dissipation term. *CFD Letters*, 15(12): 77-106.
<https://doi.org/10.37934/cfdl.15.12.77106>
- [51] Berkache, A., Amroune, S., Golbaf, A., Mohamad, B. (2022). Experimental and numerical investigations of a turbulent boundary layer under variable temperature gradients. *Journal of the Serbian Society for Computational Mechanics*, 16(1): 1-15.
<https://doi.org/10.24874/jsscm.2022.16.01.01>